Geoacoustic modeling of deep-sea carbonate sediments[a)]

Phillip Milholland, Murli H. Manghnani, Seymour O. Schlanger, and George H. Sutton

Hawaii Institute of Geophysics, University of Hawaii, Honolulu, Hawaii 96822
(Received 12 February 1980; accepted for publication 11 August 1980)

A systematic study has been made of physical and acoustic properties of 269 DSDP core samples representing a complete ooze-chalk-limestone sequence on the Ontong–Java Plateau (sites 288 and 289) and a sequence of clay-rich carbonate sediments in the Coral Sea Basin (site 210). Gradational increases in density (ρ), compressional velocity (V_p), shear velocity (V_s), compressional and shear velocity anisotropies (A_p, A_s: horizontal velocities faster than vertical velocities), and shear velocity orientation anisotropy (A_{so}: horizontally propagated shear velocities are faster when the particle motion is horizontal rather than vertical) are directly related to increasing depth (subbottom) and diagenetic stage. Silica enrichment increases ρ, V_p, and V_s but does not significantly affect A_p and A_s. Clay enrichment, on the other hand, decreases ρ, V_p, and V_s and increases A_p and, to a greater degree, A_s. It is found that $A_p > A_s$ in carbonate sediments, whereas $A_s > A_p$ in clay-rich sediments. Viable models are discussed to explain observed velocity anisotropy. Laboratory measurements agree with two previously published velocity-depth functions determined by seismic wide-angle measurements. A derived geoacoustic model accounts for the observed property-depth-diagenesis relationship for the first 1000 m of the ooze-chalk-limestone sequence, and predicts values of ρ, V_p, V_s, porosity (ϕ), Poisson's ratio (σ), shear modulus (μ), A_p, A_s, and A_{s0}.

PACS numbers: 43.30.Bp, 43.30.Dr, 92.10.Vz, 43.40.Ph

INTRODUCTION

The Ontong–Java Plateau (Fig. 1), Central Pacific Ocean, a classical area of rapid carbonate sedimentation with low terrigenous input, has one of the thickest and most complete ooze–chalk–limestone sequences: 800–1200 m thick (see Berger *et al.*[1]). Carbonate sediments also occur in the Coral Sea Basin along with terrigeneous clay-enriched carbonates and noncalcareous clays.

Laboratory investigations of physical and acoustic properties of marine sediments have proven to be of utmost value in proposing geoacoustic model(s) of the upper sedimentary layer of oceanic crust.[2–4] The present study investigates 269 samples from DSDP sites 288 and 289 in the Ontong–Java Plateau, and site 210 in the Coral Sea Basin.

The purpose of this study is threefold:

(1) To report laboratory measurements of density (ρ), compressional velocity (V_p), shear velocity (V_s), and velocity anisotropy for both compressional (A_p) and shear waves (A_s and A_{s0}), and to investigate interrelationships among ρ, V_p, V_s, Poisson's (σ), A_p, and A_s, and their variations with depth (subbottom), lithology, and diagenesis.

(2) To discuss models that can account for observed velocity anisotropy in terms of progressive diagenesis of sediments.

(3) To develop a geoacoustic model for the first 1000 m of a deep-sea carbonate sequence, and to compare this model to the velocity-depth curves from two previously published seismic wide-angle reflection studies over the Ontong–Java Plateau.

[a)]Hawaii Institute of Geophysics contribution No. 1082.

I. EXPERIMENTAL PROCEDURE

Density (ρ), compressional velocity (V_p), and shear velocity (V_s) are measured for 269 DSDP sediment samples. Whenever possible, V_p and V_s are measured in each of the three orthogonal directions. Averaged values of V_p and V_s are reported in all figures and tables. The depths reported are all subbottom. The samples are of two types: (1) soft sediments, protected inside plastic cylinders, and (2) hard sediments, in the form of cuboids. Samples were kept at 2 °C and, when not being measured, were wrapped in water-soaked tissues to maintain water saturation. The densities of soft sediments were calculated by dividing their weight by their volume. The densities of hard sediments were calculated by a buoyance method.[5] Velocities were measured at 22 °C with the pulse transmission technique described by Birch.[6] One-MHz barium titanate transducers were used for generating compressional and shear waves in the sediment samples. An axial pressure of ~2 bars was applied at the ends of the transducer mounting to produce a good acoustic contact. A mercury delay line[6] was employed for measuring pulse transmission time. The precision of velocity values reported is considered to be ±2%. Shear velocities were measured for hard sediments only.

II. DATA

Site 288

Figure 2 is a composite plot of ρ, V_p, A_p, A_s, A_{s0}, and lithology versus depth for site 288. Calcium carbonate content of sediments from site 288 decreases with depth (from 100% to 25%[7]) because of increasing amounts of chert, volcanic ash, and tuff.[8] Values of ρ, V_p, and V_s increase gradationally with depth in subunits 1A and 1B, and decrease in subunit 2A below the inferred Eocene chert horizon. Sediments of subunits 2B, 2D, and 2E become generally more lithified and siliceous with depth, resulting in average but irregular increases in

 0001-4966/80/111351-10$00.80

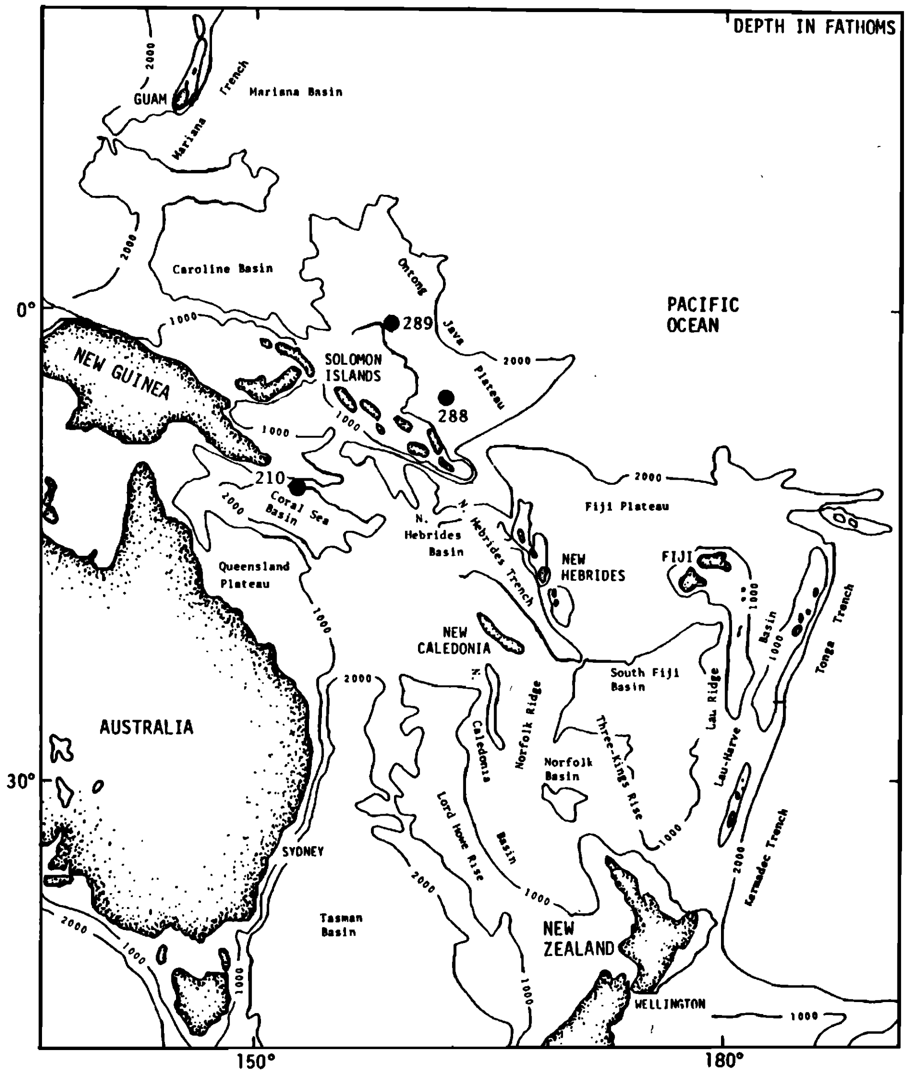

FIG. 1. Location of DSDP sites 210, 288, and 289 (after Andrews *et al.*, Ref. 8).

ρ, V_p, and V_s. Anisotropy values are close to zero for shallow sediments and increase with depth and lithification.

Site 289

Figure 3 presents ρ, V_p, A_p, V_s, A_s, and lithology versus depth for site 289. Sediments from site 289 constitute one of the thickest and most complete ooze-chalk-limestone sequences drilled by the DSDP.[8] The average values of ρ, V_p, and V_s increase over the first three lithological units. Below 1018 m, where chert first appears, the values are both larger and more variable than those of units 1, 2, or 3. Below a minor hiatus (1132 m), which is the boundary between units 4 and 5, there is a decrease in ρ, V_p, and V_s that corresponds to a decrease in both lithification and silica content. Values for the four basalt samples (1262–1266 m) are also presented.

Site 210

Figure 4 presents the data for site 210. Sediments from site 210 are clay-enriched carbonates.[9] Densities and velocities are highest for predominantly carbonate sediments, and decrease with increasing clay content. A_p and A_s are variable in the section but generally increase with depth, except below 610 m where A_p decreases sharply.

III. DISCUSSION

Table I lists averaged values of ρ, V_p, and V_s for different lithologies from the three sites. Sediments of sites 288 and 289 show a uniform increase in ρ, V_p, and V_s with both increasing lithification and silica enrichment. Values of density and velocity for basalt samples from site 289 fall within values determined for Hawaiian tholeiitic basalts measured at ambient pressure.[10] Sediments from site 210 show a decrease in ρ, V_p, and V_s with decreasing carbonate and increasing clay content.

A. Velocity-density systematics

Plots of V_p versus ρ for site 289 are shown in Fig. 5 along with best-fit cubic curve. Values of ρ and V_p increase throughout the ooze-chalk-limestone transition. Basalt values (site 289) fit along a separate line. Figure 6 shows best-fit curves and the regression equations representing ρ versus V_p relationships for sites 210, 288, and 289, and that of Ludwig *et al.*[11] For a

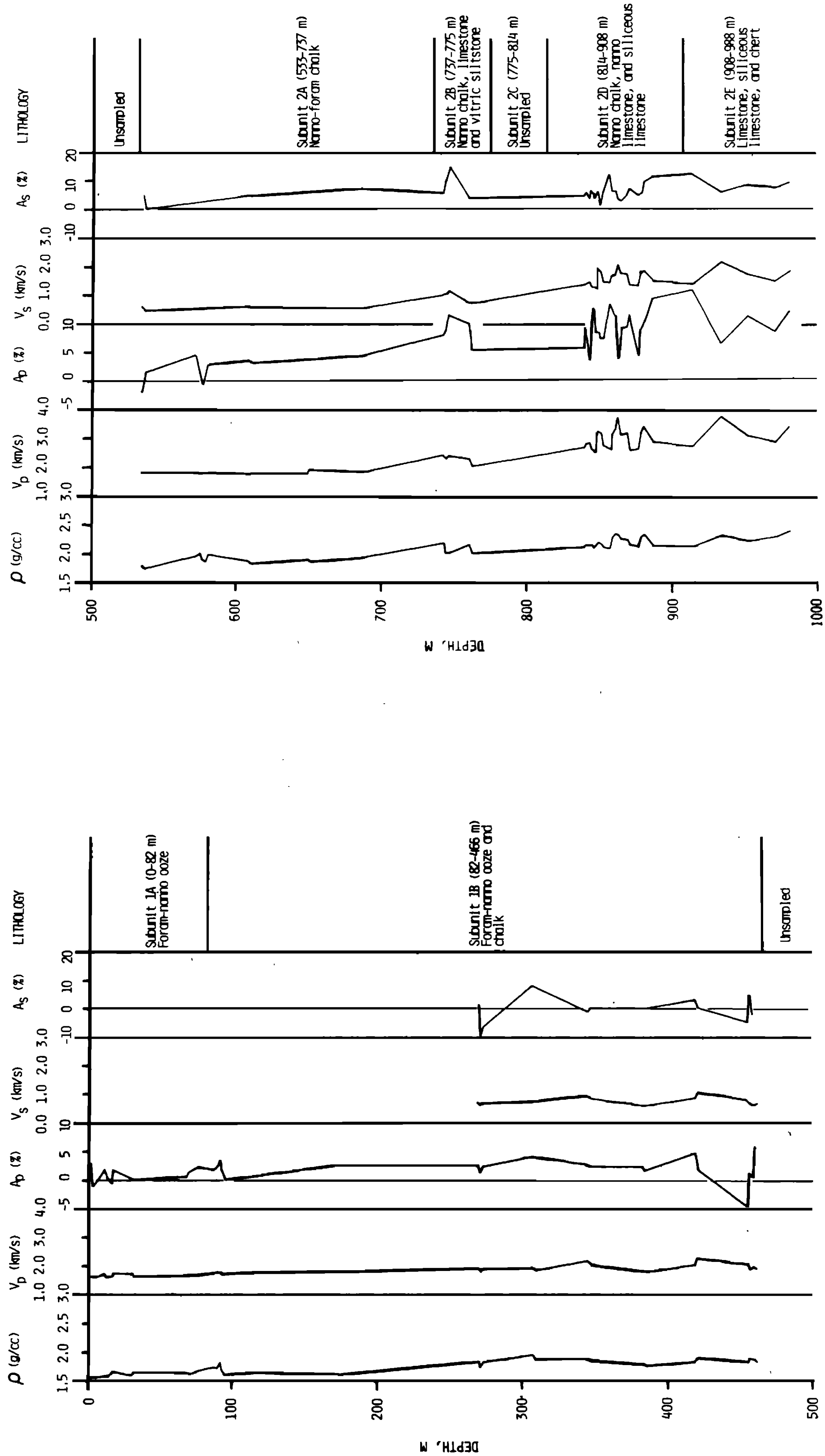

FIG. 2. Variations of ρ, V_p, A_p, V_s, A_s, and lithology with depth for DSDP site 288 sediments.

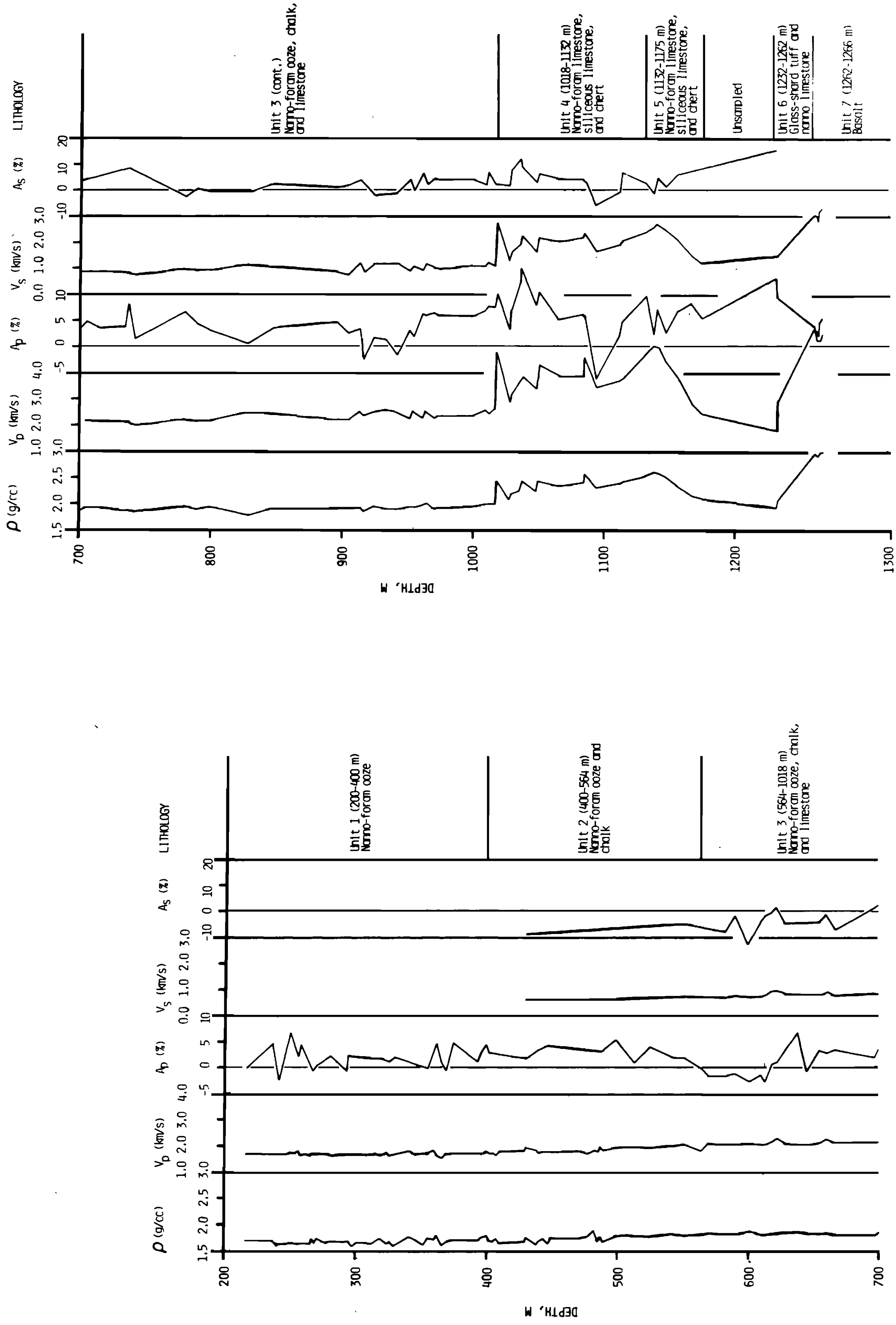

FIG. 3. Variations of ρ, V_p, A_p, V_s, A_s, and lithology with depth for site 289 sediments.

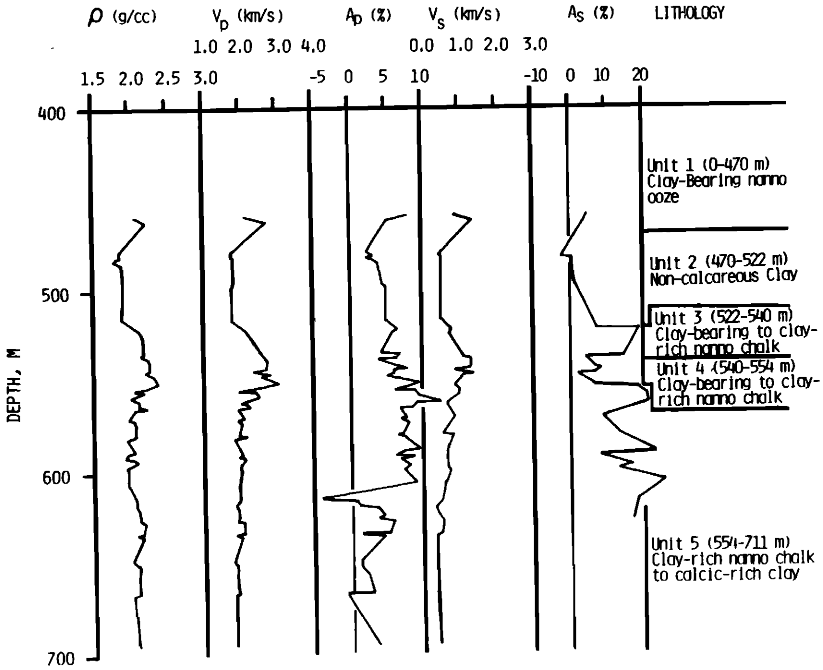

FIG. 4. Variations of ρ, V_p, A_p, V_s, A_s, and lithology with depth for DSDP site 210 sediments.

given density, clay-enriched sediments (site 210) have lower velocities than carbonate sediments (sites 288 and 289). Differences between the curves for sites 288 and 289 may be related to original differences in diagenetic potential at the two sites, or to degree and depth of chert formation, or both. Formation of chert at site 288 is more extensive and occurs at a shallower depth (~275 m) than at site 289 (~1018 m). In general, the Ludwig *et al.*[11] curve falls between the curves for clay-enriched sediments (site 210) and curves for calcareous sediments (sites 288 and 289). At higher densities, the Ludwig *et al.*[11] curve falls on the higher velocity side of all curves, including that for basalts.

Plots of V_s versus ρ for site 289 are shown in Fig. 7 along with the best-fit cubic curve. Figure 8 shows the composite relationships of V_s versus ρ curves for the three sites and that of Ludwig *et al.*[11] The relationships between V_s versus ρ show the same trends as those found for V_p versus ρ. Increases of silica and chert contents increase V_s, whereas increases of silt and clay content decrease V_s.

Ludwig *et al.*[11] presented best-fit relationships of V_p and V_s versus ρ for sedimentary rocks. They pointed out that velocity–density curves indicate general trends and not functional relationships between velocity and density. Their curves, which are widely used to predict V_p or V_s from known values of ρ, and vice versa, do not take into account differences in lithology. Our data suggest that there is a lithological dependence and that velocity–density systematics would be more accurately represented by a series of curves corresponding to different lithologies.

B. Velocity anisotropy

Marine sediments exhibit significant velocity anisotropy; values of A_p as high as 32% have been re-

TABLE I. Lithologic variations of average density, compressional velocity, and shear velocity (standard deviation in parentheses).

Lithology	% carbonate	No. of samples	$\bar{\rho}$, g/cc	$\bar{V}_p$, km/s	$\bar{V}_s$, km/s
Site 210					
Clay-bearing ooze and chalk	85–90	8	2.28 (0.16)	2.61 (0.24)	1.16 (0.20)
Clay-rich chalk	60–75	8	2.12 (0.09)	2.25 (0.22)	0.81 (0.16)
Calcic-rich clay	40–60	7	2.04 (0.09)	2.04 (0.07)	0.64 (0.06)
Noncalcareous clay	0–5	3	1.86 (0.06)	1.79 (0.04)	0.51 (0.02)
Sites 288 and 289					
Carbonate ooze		45	1.69 (0.10)	1.72 (0.08)	
Carbonate chalk		57	1.90 (0.10)	2.21 (0.27)	0.91 (0.23)
Carbonate limestone		23	2.24 (0.18)	3.19 (0.77)	1.63 (0.45)
Siliceous limestone		15	2.32 (0.15)	3.63 (0.61)	1.99 (0.31)
Chert		4	2.29 (0.06)	3.53 (0.31)	1.95 (0.26)
Basalt		4	2.92 (0.03)	5.82 (0.24)	3.16 (0.14)

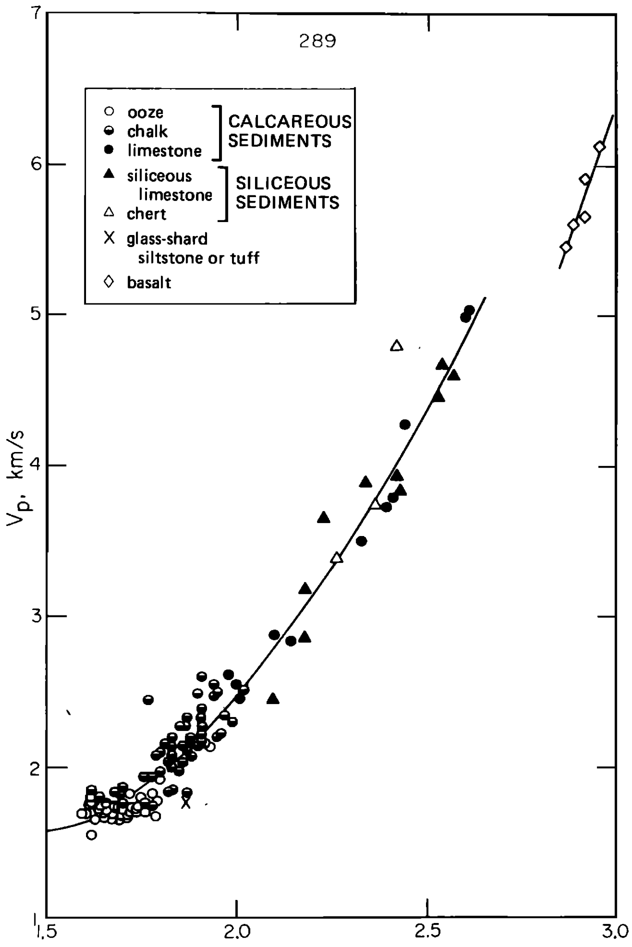

FIG. 5. V_p versus ρ for DSDP site 289. The regression equation is $V_p = 10.04 - 13.32\,\rho + 6.13\,\rho^2 - 0.68\,\rho^3$; SE = ±0.15.

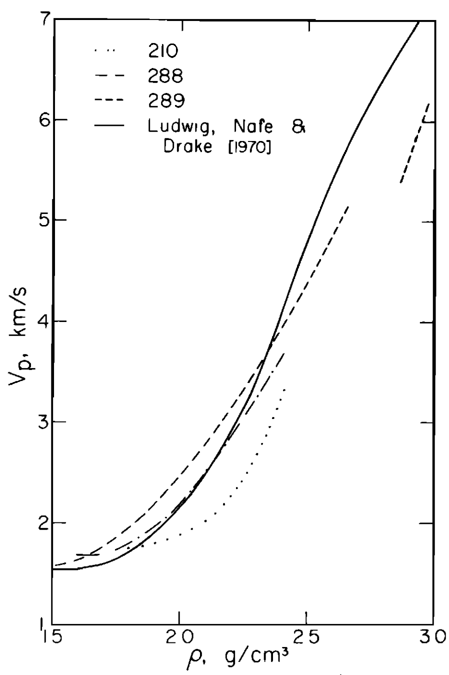

FIG. 6. V_p versus ρ. Site 210: $V_p = -56.27 + 91.88\,\rho - 48.71\,\rho^2 + 8.66\,\rho^3$; SE = ±0.17. Site 288: $V_p = 19.06 - 24.42\,\rho + 10.42\,\rho^2 - 1.21\,\rho^3$; SE = ±0.19. Site 289: $V_p = 10.04 - 13.32\,\rho + 6.13\,\rho^2 - 0.68\,\rho^3$; SE = ±0.15.

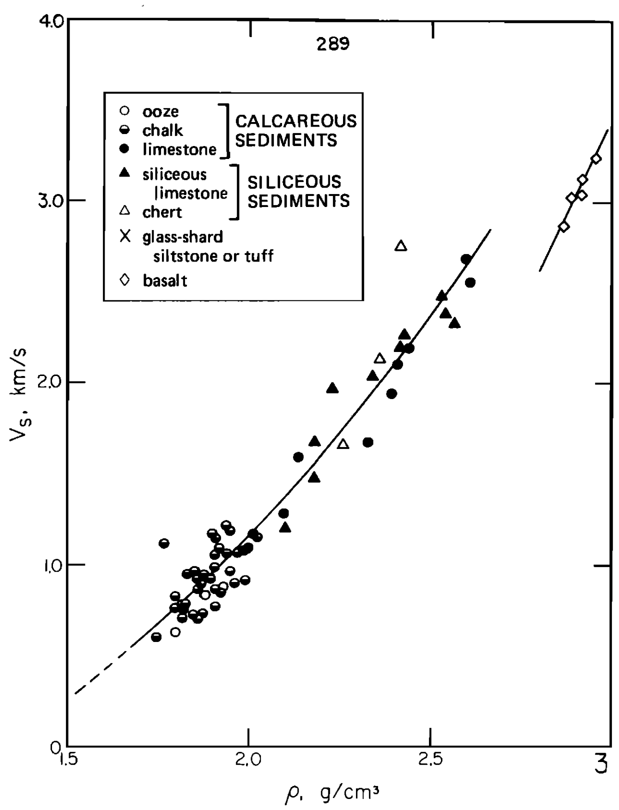

FIG. 7. V_s versus ρ for DSDP site 289. The regression equation is $V_s = -0.58 - 0.38\,\rho + 0.63\,\rho^2$; SE = ±0.15.

ported.[8,12–15] The shipboard A_p values measured by Andrews *et al.*[8] for sediments from DSDP sites 288 and 289 ranged from 0% to 10% and increased with depth. Carlson and Christensen[13] also found that A_p increases with depth and suggested that this increase could result from the vertical alignment of calcite c axes during compaction, cementation, and recrystallization.

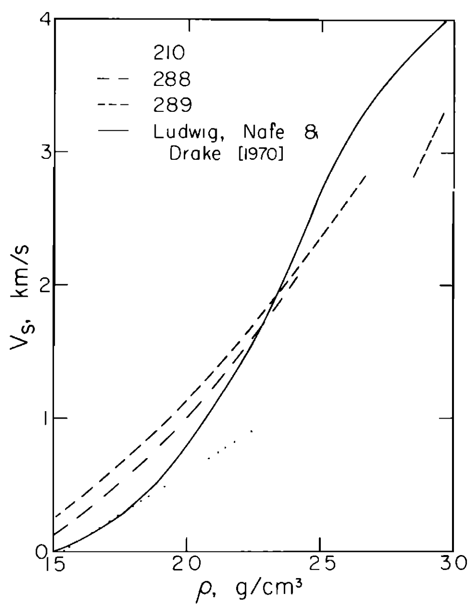

FIG. 8. V_s versus ρ. Site 210: $V_s = -1.95 + 1.28\,\rho$; SE = ±0.24. Site 288: $V_s = 0.15 - 1.37\,\rho + 0.90\,\rho^2$; SE = ±0.22. Site 289: $V_s = -0.58 - 0.38\,\rho + 0.63\,\rho^2$; SE = ±0.15.

In this study, V_p and V_s are measured for waves propagated in each of three orthogonal directions. Horizontal velocities are generally faster than vertical velocities. Anisotropy is calculated with the following equation:

$$A=[(\bar{V}_h-\bar{V}_v)/\bar{V}]\times 100\%,$$

where A = velocity anisotropy (A_p or A_s), $\bar{V}_h$ = average horizontal velocity, $\bar{V}_v$ = average vertical velocity, and $\bar{V}$ = average velocity.

For shear waves, both direction of propagation and direction of particle motion must be considered. For waves propagated in each of the three orthogonal axes, V_s is measured with particle motion parallel to the two perpendicular axes (six V_s measurements for each sample). An additional shear velocity anisotropy is related to the direction of particle motion. Horizontally propagated shear velocities are larger when the particle motion is horizontal rather than vertical. An implication of shear velocity orientation anisotropy (A_{s0}) is that shear waves propagated in the same direction but with different particle motions will travel at different speeds and will therefore tend to disperse. A_{s0} is calculated with the following equation

$$A_{s0}=[(\bar{V}_s^{hh}-\bar{V}_s^{hv})/\bar{V}_s^{h}]\times 100\%,$$

where A_{s0} = shear velocity orientation anisotropy, $\bar{V}_s^{hh}$ = average velocity of horizontally propagated shear waves with horizontal particle motion, $\bar{V}_s^{hv}$ = average velocity of horizontally propagated shear waves with vertical particle motion, and $\bar{V}_s^{h}$ = average velocity of all horizontally propagated shear waves.

Table II lists average anisotropy values as a function of lithology for sites 210, 288, and 289. Anisotropy values for sites 288 and 289 increase with increasing diagenesis throughout the ooze-chalk-limestone sequence; the largest increase is between chalk and limestone. Carbonate limestones, siliceous limestones, and cherts have similar velocity anisotropy values, suggesting that silica (chert) content does not contribute significantly to velocity anisotropy. Aside from noncalcareous clays of site 210, anisotropy increases with increasing clay content. Velocity anisotropy in clay-bearing to clay-rich oozes and chalks is twice as large as in carbonate oozes and chalks at sites 288 and 289. Both A_s and A_{s0} are larger than A_p for clay-enriched sediments, whereas A_p is larger for more calcareous sediments. In addition, A_{s0} is consistently larger than A_s. These findings are not clearly understood and warrant further investigation.

Carlson and Christensen[13] suggest that velocity anisotropy in carbonate sediments is due to alignment of the calcite c axes perpendicular to bedding. Peselnick and Robie,[16] among others, measured ultrasonic velocities in single crystals of calcite and determined that velocities are slowest parallel to the c axis ($V_p=5.62$ km/s and $V_s=3.54$ km/s) and fastest parallel to the a axis ($V_p=7.34$ km/s and $V_s=4.01$ km/s). Therefore preferential vertical alignment of c axes could produce the observed anisotropies.

In discussing the pressure regime of the deep-sea floor, Hamilton[17] suggested that sediments at the sediment–seawater interface, following deposition, are in hydrostatic equilibrium and are not subject to any uniaxial stresses. Buried sediments, however, are subjected to an overburden pressure, which increases with depth of burial and must be supported by underlying sediments. Increasing overburden pressure may align coccoliths and discoasters, which could produce velocity anisotropy. According to Gartner and Bukry,[18] discs of the *Calyptrasphaera papillifera*, a modern coccolithophore, are composed of crystallites arranged with their c axes perpendicular to the plane of the disc. Bukry[19] and Black[20] indicate that discoasters and the upper shields of the *Coccolithus* and *Cyclococcolithina* placoliths are composed of calcite crystals with vertically aligned c axes. If either normal sedimentation or overburden pressure causes coccoliths and discoasters to become aligned with their long dimensions in the horizontal plane, then more c axes will be aligned in the vertical and the sample will be anisotropic.

Alignment of calcite crystals in crushed foraminifera

TABLE II. Lithologic variations of average anisotropies (standard deviation of individual measurements in parentheses).

Lithology	No. of samples	$\bar{A}_p$, %	$\bar{A}_s$, %	$\bar{A}_{s0}$, %
Site 210				
Clay-bearing ooze and chalk	8	6.2(1.4)	6.6(3.7)	9.6(4.5)
Clay-rich chalk	8	6.8(2.6)	14.2(5.9)	9.2(6.4)
Calcic-rich clay	7	8.1(1.2)	17.4(5.0)	23.0(5.6)
Noncalcareous clay	3	3.3(1.2)	−0.4(2.4)	12.2(6.7)
Sites 288 and 289				
Carbonate ooze	48	2.0(2.1)		
Carbonate chalk	57	2.9(3.3)	0.5(4.7)	2.7(4.2)
Carbonate limestone	23	8.0(4.7)	6.2(4.9)	7.9(4.7)
Siliceous limestone	15	8.6(3.7)	5.6(3.4)	5.9(4.0)
Chert	4	8.3(2.3)	6.3(2.0)	6.2(3.7)
Basalt	4	2.5(1.0)		

may also produce anisotropy. Most of the foraminifera from sites 288 and 289 belong to the superfamily *Globigerinacea*[8] that are composed of "double walls of lamellar radial hyaline calcite" crystals.[21] Compaction and crushing of foraminifera increases with depth of burial and may result in differential alignment of c axes. This would cause anisotropy with increasing depth.

The overburden pressure would also result in dissolution and/or precipitation and enlargement of differentially aligned calcite crystals. Schlanger and Douglas[22] found that smaller coccoliths and weaker planktonic foraminifera are dissolved differentially to provide calcite for growth of larger crystals. They suggested that the driving force behind this dissolution–precipitation process is the decrease in surface area and thus a decrease in Gibbs' free energy. If dissolution is a function of c-axis alignment as well as crystal size, then dissolution may cause crystal alignment. Calcite overgrowths and cementation can also produce differential crystal alignment. Kamb[23] found that the stablest crystal orientation has the weakest axis aligned parallel to the axis of greatest compressive stress. Precipitated calcite crystals will therefore favor vertical c-axis orientation. Increasing overburden pressure and depth of burial will dissolve smaller coccolith and weaker foraminifera tests, especially those with horizontal c axes, whereas crystals with vertical c axes will be differentially precipitated and/or enlarged.

Anisotropy may be caused by: (1) alignment of discoasters and coccoliths, (2) crushing of foraminifera, and/or (3) differential crystal overgrowth and cementation. These processes may work together to produce vertical alignment of calcite c axes. Alignment of anisotropic calcite crystals with increasing depth of burial can account for the increase of anisotropy observed in the ooze-chalk-limestone sequence.

C. Effects of clay enrichment on anisotropy

Clay enrichment in calcareous sediments causes an increase in velocity anisotropy. On the other hand, noncalcareous clay sediments show lesser anisotropy (see Table II). The observed increase of anisotropy with increasing clay content may be associated with a process recognized by Weyl.[24] In this process, clay-size particles act as a catalyst in the pressure solution of carbonate sediments. As clay particles form a film between larger calcite grains, they increase the rate of diffusion by reducing the point-to-point contacts and increasing the total reactive surface of carbonate grains. The pressure-solution process should result in calcite c axes being preferentially oriented in the vertical direction, i.e., parallel to the overburden pressure. Thus an increase in the clay content of carbonate sediments will increase the pressure-solution process, and consequently increase the velocity anisotropy. Noncalcareous clays have a smaller velocity anisotropy due to the fact that no carbonate material is present and the pressure-solution process does not occur. Velocity anisotropy of noncalcareous clays is a result of preferred orientation of the clay particles parallel to the sea floor.

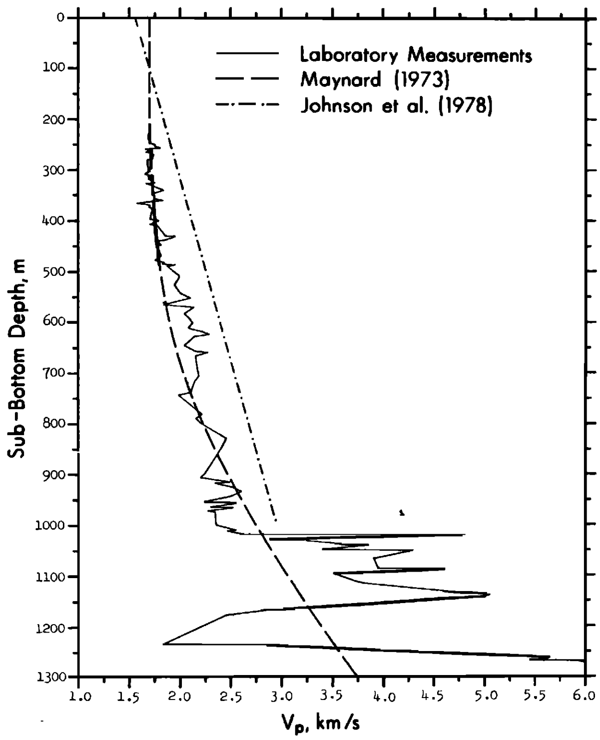

FIG. 9. Comparison of laboratory and seismic wide-angle reflection measurements of V_p.

D. Comparison with seismic reflection data

Figure 9 compares the laboratory measurements to the velocity-depth curves Maynard[25] and Johnson *et al.*[26] calculated for the Ontong–Java Plateau from seismic wide-angle reflection techniques. The averaged laboratory measurements (±2%) are minimum values that are lower than *in situ* values because of relief of intergranular (overburden) and hydrostatic pressure, elastic rebound of the samples in porosity, and temperature differences. Still, the laboratory measurements show a close fit to the seismic velocity-depth curves.

E. Geoacoustic model

Schlanger and Douglas[22] presented a model to account for the diagenetic transformation of carbonate sediments from ooze to chalk to limestone. The model takes into account the following observations: (1) rapid reduction of porosity from 80% to 65% in the first 200 m followed by more gradual reduction to 40% by 1000 m; (2) breakage, dissolution, and gradual disappearance of foraminifera, particularly thin-walled, porous, planktonic foraminifera; (3) disaggregation and dissolution of smaller coccoliths; (4) reprecipitation of this dissolved calcite as overgrowths of calcite crystals on discoasters and larger coccoliths, or interstitial cement, and/or calcite infillings of more robust benthonic foraminifera; and (5) an increase of both density and compressional velocity with depth.

A geoacoustic model (Fig. 10) was developed to match the experimental data from site 289. The Schlanger and Douglas[22] model was based on the carbonate sequence of the Magellan Rise sampled at DSDP site 167. The onset

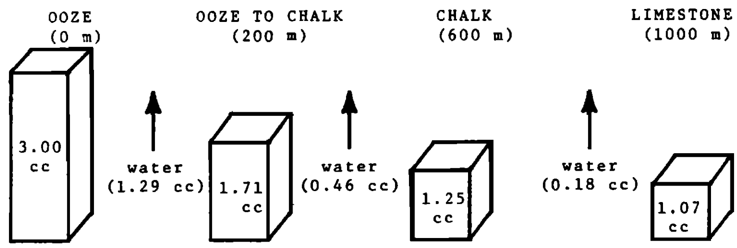

	Ooze (0 m)	Ooze to chalk (200 m)	Chalk (600 m)	Limestone (1000 m)
Density, g/cc	1.35	1.60	1.82	1.95
Compressional velocity, km/s	1.56	1.64	2.01	2.33
Shear velocity, km/s	0.06	0.42	0.82	1.07
Porosity, %	80	65	52	44
Poisson's ratio, dimensionless	.499	.465	.400	.366
Shear modulus, kilobars	0.1	2.8	12.2	22.3
A_p, %	0.0	2.0	2.9	8.0
A_s, %	0.0	0.3	0.5	6.2
A_{so}, %	0.0	1.9	2.7	7.9

FIG. 10. Geoacoustic model for carbonate sediments.

of the chalk and limestone phases occurs at shallower depths at site 167 than at site 289. Our shallowest sample was at 217 m (subbottom), so we assume the same volume and densities at 0 and 200 m as in the Schlanger and Douglas[22] model. Densities at 600 and 1000 m were calculated by carrying out a linear regression of laboratory ρ versus depth data between 600 and 1000 m [$\rho = 1.66 + 2.88\times 10^{-4} d(\mathrm{m})$; $r^2 = 0.49$]. From these densities, the appropriate volumes and amount of expelled water were calculated by using a carbonate conservate model.

V_p and V_s are calculated from density values using the regression equations of site 289, relating V_p and V_s to ρ:

$$V_p = 10.04 - 13.32\rho + 6.13\rho^2 - 0.68\rho^3;\quad SE \pm 0.19$$

$$V_s = -0.58 - 0.38\rho + 0.63\rho^2;\quad SE \pm 0.15.$$

Note that the shallowest V_p and V_s measurements were at 217 and 430 m, respectively. V_p and V_s values at 0 and 200 m are extrapolated. Porosities (ϕ) are calculated from the Nafe and Drake[27] equation:

$$\rho = 2.68 - 1.65\phi .$$

Both Poisson's ratio (σ) and shear modulus (μ) are calculated from the isotropic elasticity equations. Predicted values of A_p, A_s, and A_{s0} are 0% at 0 m, which is in agreement with results of Johnson *et al.*,[28] who determined A_p to be essentially 0% for the surface sediments of the Ontong–Java Plateau. Anisotropy values for 200, 600, and 1000 m are based on the measured averages (Table II). The volumes of chalk and limestone produced by diagenesis of an original ooze are calculated from porosity.

IV. CONCLUSIONS

A general progression, with depth, from ooze to chalk to limestone within a carbonate section is consistent with general increases, with depth, in average ρ from 1.69 to 1.90 to 2.24 g/cc, V_p from 1.72 to 2.21 to 3.19 km/s, and A_p from 2.0 to 2.9 to 8.0% (Tables I and II). In grading from chalk to limestone, V_s varies from 0.91 to 1.63 km/s, A_s from 0.5 to 6.2%, and A_{s0} from 2.7 to 7.9%. Silica enrichment results in larger average values for ρ, V_p, and V_s but does not significantly affect velocity anisotropy. Clay enrichment causes significant increases in anisotropy, possibly because of a catalytic effect on the pressure solution of calcite. A more detailed study of changes in fossils, chemistry, and mineralogy is needed to determine exact relationships between lithification, silica enrichment, clay enrichment, and changes in acoustic properties.

In addition to accounting for the state of fossil preservation and textural changes discussed by Schlanger and Douglas,[22] the geoacoustic model for pure carbonate sediments (Fig. 10) accounts for the following: Decrease in ϕ and increases in ρ, V_p, and V_s with depth, and increasing velocity anisotropy (A_p, A_s, and A_{s0}) with depth caused by vertical alignment of calcite c axes.

The geoacoustic model proposed can predict values of ρ, V_p, V_s, density and velocity gradients, ϕ, σ, μ, A_p, A_s, and A_{s0} down to a depth of burial of 1000 m for the Ontong–Java Plateau, and possibly for other areas of high carbonate sedimentation. The geoacoustic model can also be used to predict approximate depths of reflectors from reflection records.

Many widespread reflectors are revealed by air gun seismic surveys.[9,8] If ρ and V_p values in the sediment sequence below the Ontong–Java Plateau increase smoothly with depth of burial, as predicted by the geoacoustic model, there will be no reflectors. The measured values, however, deviate from the model values. These deviations are caused by variations in the diagenetic potential of carbonate layers that result from paleo-oceanographic changes.[22,29] The numerous reflectors are due either to large impedance mismatches, or to frequency dependent interference patterns resulting from small changes in ρ and V_p. A valuable experiment would be one in which frequencies are varied to see how the reflection profiles change and to determine if the reflectors are interference patterns. If the reflectors are interference patterns, then the small changes in ρ and V_p are uniform and very widespread. It would also be valuable to do a more detailed, systematic study of carbonate sections responsible for the observed reflections.

ACKNOWLEDGMENTS

This research was supported by the US Department of the Navy, Office of Naval Research. We thank the Deep Sea Drilling Project, especially Pat Paluso, Ellen Moore, J. S. Harrington, and Trudy Wood, for obtaining the samples. Thanks are also due Edwin Hamilton for his encouragement and helpful discussion concerning this research and for reviewing the manuscript.

[1]W. H. Berger, T. C. Johnson, and E. L. Hamilton, "Sedimentation on Ontong–Java Plateau: Observations on a classic 'carbonate monitor,'" in *The Fate of Fossil Fuel* CO_2 *in the Oceans*, edited by N. R. Anderson and A. Malahoff (Plenum, New York, 1977), pp. 543–567.

[2]E. L. Hamilton, "Elastic properties of marine sediments," J. Geophys. Res. **76**, 579–604 (1971).

[3]E. L. Hamilton, "Geoacoustic models of the sea floor," in *Physics of Sound in Marine Sediments*, edited by L. Hampton (Plenum, New York, 1974), pp. 181–221.

[4]E. L. Hamilton, "Geoacoustic modeling of the sea floor," Proceedings of NORDA Workshop: "Interpretative modeling of deep-ocean sediments and their physical properties," J. Acoust. Soc. Am. **68**, 1313–1350 (1980).

[5]ASTM Committee C–14, Subcommittee 4, Draft No. 3, 1971.

[6]F. Birch, "The velocity of compressional waves in rocks to 10 kilobars, Part 1," J. Geophys. Res. **64** (4), 1083–1102 (1960).

[7]I. Zemmels, H. E. Cook, and J. C. Matti, "X-ray mineralogy data, Tasman Sea and far Western Pacific," in *Initial Reports of the Deep Sea Drilling Project*, Vol. 30, edited by J. E. Andrews *et al.*, (US GPO, Washington, DC, 1975), pp. 603–616.

[8]J. E. Andrews, G. Packham, *et al.*, *Initial Reports of the Deep Sea Drilling Project*, Vol. 30 (US GPO, Washington, D.C., 1975), 753 pp.

[9]R. E. Burns, J. E. Andrews, *et al.*, *Initial Reports of the Deep Sea Drilling Project*, Vol. 21 (US GPO, Washington, DC, 1973), 931 pp.

[10]M. H. Manghnani and G. P. Woollard, "Elastic wave velocities in Hawaiian rocks at pressures to ten kilobars," in *The Crust and Upper Mantle of the Pacific Area*, Geophys. Monogr. Ser., Vol. 12, edited by L. Knopoff, C. L. Drake, and P. J. Hart (AGU Washington, DC, 1968), pp. 501–516.

[11]W. J. Ludwig, J. E. Nafe, and C. L. Drake, "Seismic refraction," in *The Sea*, Vol. 4, Part 1, edited by M. Hill, E. Goldberg, A. Maxwell, and W. Munk (Interscience, New York, 1970), pp. 53–84.

[12]B. E. Tucholke, N. T. Edgar, and R. E. Boyce, "Physical properties of sediments and correlations with acoustic stratigraphy, Leg 35, Deep Sea Drilling Project," in *Initial Reports of Deep Sea Drilling Project*, Vol. 35, edited by C. D. Hollister *et al.* (US GPO, Washington, DC, 1976), pp. 229–249.

[13]R. L. Carlson and N. I. Christensen, "Velocity anisotropy in semi-indurated calcareous deep sea sediment," J. Geophys. Res. **84**, 205–211 (1979).

[14]P. D. Milholland, "Geoacoustic Model of Deep Sea Carbonate Sediments," M. S. thesis, Univ. of Hawaii, Honolulu (1978).

[15]R. T. Bachman, "Acoustic anisotropy in marine sediments and sedimentary rocks," J. Geophys. Res. **84**, (B13), 7661–7663 (1979).

[16]L. Peselnick and R. A. Robie, "Elastic constants of calcite," J. Appl. Phys. **34**, 2494–2495 (1963).

[17]E. L. Hamilton, "Consolidation characteristics and related properties of sediments from experimental mohole (Guadalupe site)," J. Geophys. Res. **69**, 4257–4269 (1964).

[18]S. Gartner, Jr., and D. Bukry, "Tertiary holococcoliths," J. Paleontol. **43**, (5), 1213–1221 (1969).

[19]D. Bukry, "Cenozoic calcareous nannofossils from the Pacific Ocean," Trans. San Diego Soc. Nat. Hist. 16 (14), 303–328 (1971).

[20]M. Black, "Crystal development in Discoasteraceae and Braarudosphaeraceae (planktonic algae)," Paleontology **15**, Part 3, 476–489 (1972).

[21]A. R. Loeblich, Jr., and H. Tappan, *Treatise on Invertebrate Paleontology, Part C Protista 2, Sarcodina, Chiefly "Thecamoebians" and Foraminiferida*, Vol. 2, edited by R. C. Moore (G.S.A. and the University of Kansas Press, Lawrence, 1964), p. C652.

[22]S. O. Schlanger and R. G. Douglas, "The pelagic ooze-chalk-limestone transition and its implication for marine stratigraphy," Spec. Publ. Int. Assoc. Sedimentol. **1**, 117–148 (1974).

[23]W. B. Kamb, "Theory of preferred crystal orientation developed by crystallization under stress," J. Geol. **67**, 153–170 (1959).

[24]P. K. Weyl, "Pressure solution and the force of crystallization—A phenomenological theory," J. Geophys. Res. **64** (11), 2001–2025 (1952).

[25]G. L. Maynard, "Seismic Wide-Angle Reflection and Refraction Investigation of the Sediments on the Ontong–Java Plateau, Ph.D. Thesis, Univ. of Hawaii, Honolulu (1973).

[26]T. C. Johnson, E. L. Hamilton, R. T. Bachman, and W. H. Berger, "Sound velocities in calcareous oozes and chalks from sonobuoy data: Ontong–Java Plateau, western equatorial Pacific," J. Geophys. Res. **83**, 283–288 (1978).

[27]J. E. Nafe and C. L. Drake, "Physical properties of marine sediments," in *The Sea*, edited by M. N. Hill (Interscience, New York, 1963), pp. 794–813.

[28]T. C. Johnson, E. L. Hamilton, and W. H. Berger, "Physical properties of calcareous ooze: Control by dissolution at depth," Mar. Geol. **24**, 259–277 (1977).

[29]W. H. Berger and L. A. Mayer, "Deep sea carbonates: Acoustic reflectors and lysocline fluctuations," Geology **6**, 11–15 (1978).